Mesospheric N2O enhancements as observed by MIPAS on Envisat during the polar winters in 2002?2004

B. Funke, M. López-Puertas, M. García-Comas, G. P. Stiller, T. von Clarmann, N. Glatthor

**Atmospheric
Chemistry
and Physics
Discussions**

ACPD

8, 10561–10596, 2008

**Mesospheric N$_2$O
enhancements
observed by MIPAS**

B. Funke et al.

Title Page

Abstract	Introduction
Conclusions	References
Tables	Figures

◄◄   ►►

◄   ►

Back   Close

Full Screen / Esc

Printer-friendly Version

Interactive Discussion

Mesospheric N$_2$O enhancements as observed by MIPAS on Envisat during the polar winters in 2002–2004

B. Funke[1], M. López-Puertas[1], M. García-Comas[1], G. P. Stiller[2], T. von Clarmann[2], and N. Glatthor[2]

[1]Instituto de Astrofísica de Andalucía (CSIC), Granada, Spain
[2]Forschungszentrum Karlsruhe, Institut für Meteorologie und Klimaforschung (IMK), Karlsruhe, Germany

Abstract

N_2O abundances ranging from 0.5 to 6 ppbv were observed in the polar upper strato-sphere/lower mesosphere by the MIPAS instrument on the Envisat satellite during the Arctic and Antarctic winters in the period July 2002 to March 2004. A detailed study of the observed N_2O–CH_4 correlations shows that such enhancements are of chemical rather than dynamical origin. The N_2O enhancements observed at 58 km occurred in presence of NO_x intrusions from the upper atmosphere which were related to energetic particle precipitation. Further, the inter-annual variability of mesospheric N_2O correlates well with observed precipitating electron fluxes. The analysis of possible chemical production mechanisms shows that the major part of the observed N_2O enhancements is most likely generated under dark conditions by the reaction of NO_2 with atomic nitrogen at altitudes around 70–75 km in the presence of energetic particle precipitation. A possible additional source of N_2O in the middle and upper polar atmosphere is the reaction of $N_2(A^3\Sigma_u^+)$, generated by precipitating electrons, with O_2, which would lead to N_2O production peaking at altitudes around 90–100 km. N_2O produced by the latter mechanism could then descend to the mesosphere and upper stratosphere during polar winter.

1 Introduction

Nitrous oxide is the main precursor of odd nitrogen in the middle atmosphere. Its major sources, both natural and man-made, are located at the surface from where it is transported into the stratosphere. Photolysis by solar UV is its major sink and the reaction with $O(^1D)$ leads to the formation of NO.

Due to its long chemical lifetime and the apparent absence of sources in the middle atmosphere, N_2O is an excellent tracer for stratospheric transport processes. In particular, correlations of observed N_2O abundances with other tracers such as CH_4 or CFCs have been widely used in transport studies (Michelsen et al., 1998a; Plumb

et al., 2000; Ray et al., 2002).

Recently, however, Funke et al. (2008) reported polar stratospheric and mesospheric N_2O enhancements in the Northern hemisphere (NH) in the aftermath of the large solar proton event (SPE) which took place in October–November 2003. These N_2O enhancements were attributed to chemical production of N_2O by

$$NO_2 + N(^4S) \rightarrow N_2O + O. \tag{R1}$$

Both species were largely enhanced as a consequence of ionization caused by solar protons. Semeniuk et al. (2007)[1] reported polar mesospheric N_2O enhancements in the NH observed by the Fourier Transform Spectrometer on SCISAT-1 during February–April 2004 which were also attributed to the reaction of NO_2 and atomic nitrogen. Since no major SPE occurred in this period, these authors assumed that enhanced N abundances, required for the formation of N_2O, were generated by ionization caused by auroral electron precipitation.

An alternative production mechanism of middle and upper atmospheric N_2O was proposed by Zipf and Prasad (1980): i.e., metastable $N_2(A^3\Sigma_u^+)$ is produced by electron impact during auroral substorms and reacts with O_2 to form N_2O:

$$N_2(A^3\Sigma_u^+) + O_2 \rightarrow N_2O + O. \tag{R2}$$

In accordance with laboratory measurements (Zipf, 1980), these authors considered an efficiency of 0.6 to form N_2O by the reaction of $N_2(A^3\Sigma_u^+)$ with molecular oxygen, which would then result in production of enormous amounts of N_2O around 90–100 km during geomagnetic perturbations. However, the observation of such a high efficiency for producing N_2O by Reaction (R2), initially reported by Zipf (1980), has not been confirmed by other groups, and the branching ratio for this channel is probably less than 0.02 (de Sousa et al., 1985; Iannuzzi et al., 1982).

---

[1]Semeniuk, K., McConnell, J. C., Jin, J. J., Jarosz, J. R., Boone, C. D., and Bernath, P. F.: N_2O production by high energy auroral electron precipitation, J. Geophys. Res., submitted, 2007.

Mesospheric N_2O enhancements observed by MIPAS

B. Funke et al.

Title Page

Abstract | Introduction

Conclusions | References

Tables | Figures

|◄ | ►|

◄ | ►

Back | Close

Full Screen / Esc

Printer-friendly Version

Interactive Discussion

Here, we report upper stratospheric and mesospheric N_2O enhancements observed by the Michelson Interferometer for Passive Atmospheric Sounding (MIPAS) instrument on Envisat in polar winters during 2002–2004. In Sect. 2, we present the observed spatial distributions of polar winter N_2O and their temporal evolution. The chemical origin of these N_2O enhancements is demonstrated in Sect. 3 by means of an analysis of N_2O-CH_4 tracer-tracer correlations, and possible production mechanisms are discussed in Sect. 4.

2   MIPAS observations and data analysis

MIPAS is a limb emission Fourier transform spectrometer designed for the measurement of trace species from space (Fischer and Oelhaf, 1996; European Space Agency, 2000; Fischer et al., 2007). It is part of the instrumentation of the Environmental Satellite (ENVISAT) which was launched into its sun-synchronous polar orbit of 98.55°N inclination at about 800 km altitude on 1 March 2002. MIPAS operated from July 2002 to March 2004 at full spectral resolution of $0.035\,\mathrm{cm}^{-1}$ (unapodized) in terms of full width at half maximum and has resumed operation with reduced resolution, after an instrument failure, since August 2004. MIPAS observes the atmosphere during day and night with global coverage from pole to pole. Within its standard observation mode at full spectral resolution, MIPAS covers the altitude range from nominally 68 km down to 6 km with tangent altitudes at 68, 60, 52, 47, and then at 3 km steps from 42 to 6 km. Occasionally, MIPAS also operates in several upper atmospheric measurement modes scanning up to 170 km. The field of view of MIPAS is 30 km in the horizontal and approximately 3 km in the vertical. MIPAS passes the equator in southerly direction at 10.00 a.m. local time 14.3 times a day. During each orbit up to 72 limb scans are recorded. The Level-1b processing of the data (version 4.61/62 was used here), including processing from raw data to calibrated phase-corrected and geolocated radiance spectra, is performed by the European Space Agency (ESA) (Nett et al., 1999, 2002).

2.1 Analysis of IMK/IAA-generated N_2O data

Data presented and discussed in this section are vertical profiles of abundances of N_2O and CH_4 retrieved with the scientific IMK-IAA data processor (von Clarmann et al., 2003a) developed and operated by the Institute of Meteorology and Climate Research (IMK) in Karlsruhe together with the Instituto de Astrofísica de Andalucía (IAA) in Granada. This data processor is based on a constrained non-linear least squares algorithm with Levenberg-Marquardt damping and line by line radiative transfer calculations with the Karlsruhe Optimized and Precise Radiative Transfer Algorithm (KOPRA) (Stiller et al., 2002). The first step in the L2 processing is the determination of the spectral shift, followed by the retrieval of temperature and elevation pointing (von Clarmann et al., 2003b), where pressure is implicitly determined by means of hydrostatic equilibrium. The retrieval of volume mixing ratio (vmr) profiles of species is carried out in the following order: O_3, H_2O, HNO_3, and then CH_4 and N_2O simultaneously. The results of the species firstly retrieved are used in the retrievals of the subsequent species. The N_2O vmr is retrieved from the MIPAS spectra around $1284.9\,cm^{-1}$, where the v_1 band of N_2O is located (Glatthor et al., 2005). The retrievals are performed from selected spectral regions (micro-windows) which vary with tangent altitudes in order to optimize computation time and minimize systematic errors (Echle et al., 2000). Thus, height dependent combinations of micro-windows were selected with a trade-off between computation time and total retrieval error. The retrieval noise error in the N_2O vmr is typically 3% at 10–44 km and 22% at 50 km. The total error varies between 10 and 20% at 10–35 km and is about 30% between 35–50 km (Glatthor et al., 2005). The resulting vertical resolution was about 4 km in the altitude range 15–40 km and decreased to more than 10 km below and above this region. More details on the N_2O retrieval strategy can be found in Glatthor et al. (2005).

Two data sets with different retrieval versions are used in this study: The first one includes N_2O and CH_4 data (Version V3O_8.0) and covers 45 days between 13 September 2002 and 21 October 2003. The second one was derived with an updated retrieval

Mesospheric N_2O enhancements observed by MIPAS

B. Funke et al.

Title Page

Abstract	Introduction
Conclusions	References
Tables	Figures

◄◄   ►►

◄   ►

Back   Close

Full Screen / Esc
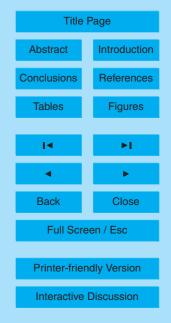
Printer-friendly Version

Interactive Discussion

version V3O_12.0 and includes 54 days between 9 September 2003 and 25 March 2004. The retrieval updates applied to the latter data set include a weaker regularization of N_2O at altitudes above 45 km in order to achieve a more realistic shape of the retrieved profiles in the presence of extraordinary mesospheric N_2O enhancements such as those found in the aftermath of the 2003 "Halloween" SPE and the Arctic winter 2004. It should be noted, however, that above 60 km, retrieved profiles of enhanced N_2O tend to be low-biased in both data sets due to the regularization. In consequence, the peak altitudes of the derived mesospheric N_2O enhancements could appear lower than in reality.

In order to analyze the retrieved trace gas profiles in a dynamical context, potential vorticity data from ECMWF analysis has been used for the representation of N_2O and CH_4 data in equivalent latitudes.

Figure 1 shows potential temperature-equivalent latitude daily mean cross sections of N_2O and CH_4 vmr on representative days in the NH winter 2002/2003, SH winter 2003, and NH winter 2003/2004. Mesospheric polar winter N_2O enhancements are clearly visible during all days, being most pronounced at equivalent latitudes higher than 60°. Their magnitudes, however, vary significantly, reaching 0.8, 1.7, and 10 ppbv on 8 December 2002, 8 June 2003, and 9 February 2004, respectively. The peak altitudes of the retrieved N_2O enhancements are located around 60 km. Due to regularization effects in the retrieval, however, it cannot be excluded that the true peak altitudes are located at higher altitudes. The corresponding CH_4 distributions show generally low vmr values at the N_2O peak positions which are typical for polar winter descent of mesospheric air. Further, lowest CH_4 vmrs appeared on 9 February 2004 when highest N_2O amounts were observed. This anti-correlation of CH_4 and N_2O at high latitudes indicates that a dynamical origin of the observed N_2O enhancements is rather unlikely. The latitudinal extension of the mesospheric N_2O layer is much narrower in February 2004 than in the other winters, showing a pronounced gradient at 60°N equivalent latitude and background N_2O abundances at lower latitudes. A strong gradient is also found in the CH_4 distributions, although with opposite sign, indicating
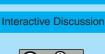
that the polar vortex boundary was located at 60°N equivalent latitudes. Indeed, an unusual strong vortex together with a very fast and efficient descent of mesospheric air has been observed in this particular Arctic winter (Manney et al., 2005). N_2O enhancements observed during the other two polar winters do not show such pronounced gradients and extend towards low latitudes, reaching background values around 30°. Thus, it seems that in the 2002-2003 winters stronger mixing of polar and tropical air occurred through a weaker polar vortex boundary.

Figure 2 shows the temporal evolution of mean N_2O and CH_4 abundances (Version V3O_8.0) within 70–90° S equivalent latitudes in the period September 2002 to November 2003. In September 2002, characterized by a major warming which led to a split of the stratospheric polar vortex (e.g., Newman and Nash, 2005), mesospheric N_2O abundances around 0.5 ppbv were observed. Given the unusual dynamical situation which allowed for intrusions of tropical air masses into the polar region, it is not clear whether these small N_2O enhancements are of chemical or dynamical origin. The apparent descent visible in the temporal evolution of N_2O and CH_4 abundances during the following polar summer (i.e. December to April) is originated by photochemical losses of both species involving photolysis and reactions with OH and $O(^1D)$. Later on, a tongue of enhanced CH_4 can be seen, localized around 60 km in March and descending to 30 km in July/August. These CH_4 enhancements were generated by an accelerated Brewer-Dobson circulation with strong poleward transport of tropical air masses rich in CH_4 preceding the downward motion during polar winter. The temporal evolution of N_2O shows a similar behavior, though transport-generated N_2O enhancements appear later and at lower altitudes compared to the corresponding CH_4 distributions. During June–August 2003, three N_2O peaks reaching values higher than 1 ppbv show up at altitudes around 55–65 km while CH_4 vmrs were generally low due to polar winter descent. As already seen in the N_2O zonal mean distributions on 8 June, these N_2O peaks are most likely related to chemical production. From August until the final breakup of the polar vortex in October, CH_4 abundances started to increase above 40 km due to stronger mixing across a weakened vortex boundary (Funke et al., 2005).

These intrusions of tropical air into the polar regions makes it more difficult to distinguish whether mesospheric N_2O enhancements in August and September are related to chemistry or to transport.

The temporal evolution of mean N_2O and CH_4 abundances within 70–90°N equivalent latitudes are shown in Fig. 3 (Version V3O_8.0 covering September 2002 to November 2003) and Fig.4 (Version V3O_12.0 covering September 2003 to March 2004). The general patterns of the temporal evolution of CH_4 distributions in the NH are similar to the SH, except that during the NH Arctic winters major warmings occurred which led to pronounced polar vortex excursions towards mid-latitudes and hence, to enhanced mixing of polar and tropical air masses in the stratosphere and mesosphere in January 2003 and 2004. In consequence, high CH_4 vmrs were observed during these events. Several episodes of upper stratospheric and mesospheric N_2O enhancements were found in the Arctic winters 2002–2004. In November/December 2002, enhancements of 0.5–0.8 ppbv occurred around 60 km. As already seen in the zonal mean distributions on 8 December 2002 (Fig. 1), these N_2O enhancements went along with low CH_4 vmrs and are thus most likely of chemical origin. The mesospheric enhancements were interrupted by the warming event in January 2002, but showed up again in February inside of descending air masses with even lower CH_4 vmrs than in December 2002. Similar as in the SH, the NH polar summer 2003 was characterized by mesospheric air masses very poor in N_2O.

The temporal evolution of N_2O in the Arctic winter 2003/2004 (Fig. 4) was rather unusual due to the "Halloween" solar proton event which led to efficient and instantaneous N_2O production by Reaction (R1) of up to 5 ppbv in the 50–70 km region on 29 October 2003. As discussed in detail in Funke et al. (2008), these N_2O enhancements descended with the meridional circulation in the following weeks down to 40 km. Several smaller enhancements (up to 2 ppbv) occurred around 60 km in the second half of November and mid-December which cannot be attributed to SPEs. These enhancements disappeared by the end of December during the major warming event. Around 15 January 2004, mesospheric N_2O abundances started suddenly to increase to val-

ues up to 7 ppbv (see also Fig. 1, lower left panel), coinciding with the period where strongest polar winter descent occurred. These air masses rich in N_2O of chemical origin descended down to altitudes around 45 km until end of March 2004.

2.2 Analysis of ESA-generated N_2O data

Since episode-based scientific MIPAS-IMK-IAA data are available only for selected days, we have also analysed the operational ESA N_2O, NO_2, and CH_4 data (reprocessed data version 4.61/4.62). This further allows to corroborate the evidence for chemically-produced mesospheric N_2O enhancements found in the IMK/IAA data with data generated with an independent retrieval algorithm and, hence to exclude retrieval artifacts as a possible explanation. ESA data are retrieved with the operational retrieval algorithm as described by Raspollini et al. (2006). ESA 4.61/4.62 data include all MIPAS observations taken with full spectral resolution between June 2002 and March 2004, representing thus a quasi-continuous data set. However, care has to be taken when statistically analyzing ESA data products (i.e. zonal mean values) which are close to the detection limit since negative vmrs are not supported by this retrieval algorithm. Whenever negative vmrs occur at a given altitude during an iteration of the retrieval, the corresponding vmr profile points are set arbitrarily to a value of 10^{-10} ppmv. The rationale of this procedure is to avoid numerical retrieval instabilities. This truncation of negative values, however, results in a positive bias of ESA vmr mean values, if the "true" mean value is close to the noise error or below. In order to correct for this bias, the following procedure was applied: Assuming zonal homogeneity at a given altitude and a Gaussian distribution of N_2O measurements affected by random errors, the expectation value ε of all truncated negative values to be zonally averaged can be determined by

$$\varepsilon = \int_{-\infty}^{0} \frac{x}{\sigma\sqrt{2\pi}} \exp\left[-\frac{(x-x_0)^2}{2\sigma^2}\right] dx, \tag{1}$$

Mesospheric N_2O enhancements observed by MIPAS

B. Funke et al.

⏮ | ⏭

◀ | ▶

Back | Close

Full Screen / Esc

Printer-friendly Version

Interactive Discussion

where x_0 is the "true" zonal mean value and σ is the standard deviation assumed to be identical to the zonally averaged noise error. After determination of ε by resolving numerically the integral in Eq. (1), the corrected zonal mean can be calculated by substitution of all truncated profile points by ε and subsequent averaging. Since the "true" zonal mean value is unknown at the beginning, we start with the uncorrected value and iterate until x_0 changes by less than 2%. This convergence criterion was usually fulfilled after a few iterations.

Figure 5 shows the temporal evolution of ESA N_2O vmr averaged within 70–90° geographical latitudes at 58 km before and after the statistical correction, together with IMK/IAA-retrieved N_2O averages and mean noise errors. Excellent agreement between the corrected averaged ESA and IMK/IAA data is found, while the uncorrected ESA data shows a positive bias up to 1.2 ppbv in dependence of the noise error. We thus conclude that the statistical correction applied to the zonally averaged ESA N_2O works satisfactorily. It can further be excluded that the N_2O enhancements discussed in the previous section are generated by a retrieval artifact in any of the data sets, given that they appear with good quantitative agreement in two independently retrieved data sets.

3 Analysis of N_2O-CH_4 correlations

In the tropics and middle latitudes, N_2O and CH_4 show compact correlations, only varying little between seasons and years (Michelsen et al., 1998a,b). N_2O vmrs generally increase monotonically with increasing CH_4 with a curved relationship. In polar spring, this relationship tends to be more linear due to mixing of subsided vortex air and midlatitude air masses. Without mesospheric sources, N_2O should increase with CH_4 in any case, while the presence of such source should invert this dependence for low CH_4 vmrs. Therefore, N_2O-CH_4 correlations represent an excellent tool for the detection of mesospheric N_2O sources.

We have analyzed N_2O-CH_4 correlations determined from ESA data on a monthly

B. Funke et al.

basis, using all available observations between 45 km and 60 km within 60–90° S and 60–90° N. We first performed a histogramming of the observations within bins of $\Delta CH_4 = 10$ ppbv and $\Delta N_2O = 0.1$ ppbv. Median values of the obtained N$_2$O probability density function (PDF) at a given CH$_4$ level were then determined in a second step.

⁵ Figure 6 shows the obtained temporal evolution of the N$_2$O-CH$_4$ correlation for 60–90° S and 60–90° N. Deviations from the typical correlation, characterized by monotonically increasing N$_2$O with CH$_4$, are clearly visible in all four polar winters at CH$_4$ levels below 0.1 ppmv, providing an additional proof for mesospheric N$_2$O sources. Maximum median values of the N$_2$O PDFs of 2.2 and 4 ppbv are found at the lowest

¹⁰ CH$_4$ levels during June 2003 (month 12) in the SH and January 2004 (month 19) in the NH, respectively. During these months, a pronounced anti-correlation of N$_2$O and CH$_4$ below 0.1 ppmv was observed. During the Antarctic winter 2002 and Arctic winter 2002/2003, deviations from the typical correlation were less pronounced. In these winters, maximum median values of the N$_2$O PDFs of 1 ppbv are found at CH$_4$ levels

¹⁵ of 0.03–0.05 ppmv.

A further anomaly is found during November 2003 (month 17) in the NH, when N$_2$O was significantly increased after the "Halloween" SPE. In contrast to the perturbed polar winter correlations discussed above, however, enhanced N$_2$O is found at nearly all CH$_4$ levels. This is expected, since solar protons led to in situ production of N$_2$O

²⁰ at altitudes above 45 km. The fact that polar winter episodes of enhanced N$_2$O are characterized by inverted N$_2$O-CH$_4$ correlations at CH$_4$ levels smaller than 0.5 ppbv hints thus at descent of air masses enriched in N$_2$O from higher altitudes rather than in situ production.

Increased median values of N$_2$O PDFs at CH$_4$ levels higher than 0.1 ppmv are not

²⁵ only found in the aftermath of the "Halloween" SPE. Tongues of high N$_2$O are visible during July 2002 (month 2), June 2003 (month 12), and September 2003 (month 15) in the SH, as well as February 2003 (month 8) and January 2004 (month 19) in the NH. Such enhancements hint at mixing of descended N$_2$O-rich and CH$_4$-poor mesospheric air masses with ambient air masses from lower latitudes.

The finding that chemical production of N_2O occurred in the mesosphere during all polar winters in the period 2002–2004, though with variable magnitude, makes it rather unlikely that mesospheric N_2O enhancements are sporadic singular phenomena. It is further evident that polar N_2O-CH_4 correlations are significantly perturbed by this mesospheric N_2O source.

4 Discussion

In order to understand which are the chemical mechanisms responsible for the observed polar winter N_2O enhancements and which are the atmospheric parameters affecting their magnitudes and inter-annual variations, we have assessed the temporal evolutions of polar mesospheric N_2O, CH_4, and NO_2 at 58 km from the ESA data set, jointly with precipitating electron fluxes observed by the MEPED instrument on NOAA 16 (poes.ngdc.noaa.gov/data/avg) and calculated ion pair production rates due to solar protons (Jackman et al., 2008).

The temporal evolution of these quantities are shown in Figs. 7 and 8 for the SH and NH, respectively. In order to isolate the N_2O amount generated by the mesospheric source from the contribution of N_2O of tropospheric origin, we have estimated the latter by applying a typical N_2O-CH_4 correlation to the CH_4 observations. This correlation has been determined from an average of the monthly N_2O-CH_4 correlations presented above, excluding the polar winter periods (June–September in the SH and November–February in the NH) perturbed by mesospheric N_2O generation. A dominant contribution of tropospheric N_2O at 58 km was found in the SH polar regions from September 2002 to December 2002 and from October 2003 to January 2004. In the NH, we found smaller amounts of tropospheric N_2O with dominant contributions during the major warming in January 2003 and from April to May 2003. Except for these episodes, N_2O observed at 58 km was produced near entirely by the mesospheric source.

Possible mesospheric N_2O production mechanisms based on Reactions (R1) and (R2) rely on the availability of atomic nitrogen or metastable $N_2(A^3\Sigma_u^+)$, which are both

largely enhanced during episodes of energetic particle precipitation. It has already been demonstrated by Funke et al. (2008) that the N_2O enhancements observed after the 2003 "Halloween" SPE in the Arctic stratosphere and lower mesosphere were generated locally by Reaction (R1) in the presence of enhanced N produced under the impact of solar protons. In the following discussion, we focus on the other N_2O enhancements observed in the polar winters during 2002–2004. In order to assess whether solar protons could have played a role in these N_2O enhancements, we looked for other SPEs during this period. However, the atmospheric ionization rates due to solar protons at 0.3 hPa (Figs. 7 and 8, lower panels), which represent a direct measure of SPE-induced N production, shows only very small peaks apart of the October–November 2003 event. It is thus very unlikely that SPE-induced N_2O production had significantly contributed to the observed N_2O enhancements under discussion.
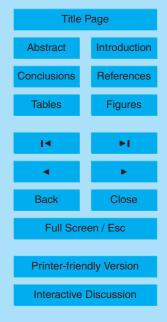
A further source of enhanced N or $N_2(A^3\Sigma_u^+)$ could be energetic electron precipitation (EEP). Precipitating electron fluxes of different energies observed by the MEPED instrument are shown in Figs. 7 and 8 (lower panels). These fluxes have been averaged over a 30-day period in order to reflect that N_2O losses are very small during polar winter and EEP-induced N_2O production would therefore tend to accumulate. Fluxes of precipitating electrons of energies 30 keV, 100 keV and 300 keV included in Figs. 7 and 8 cause ionization peaks at altitudes around 85, 75, and 60 km, respectively (Callis et al., 1998). Since only relative temporal variations of these fluxes are of interest when comparing them to the evolution of polar winter N_2O enhancements, fluxes of different energies have been scaled arbitrarily for the sake of a better representation. Electron flux increases coincident with SPEs (i.e., 29 May and 29 October 2003) should be interpreted with caution since MEPED electron measurements are compromised by the presence of protons, although SPEs are thought to be associated with elevated electron fluxes inside the polar caps.

It becomes evident from Figs. 7 and 8 that strongest N_2O enhancements at 58 km occur in polar winters with highest electron precipitation, i.e. the Antarctic winter 2003 and the Arctic winter 2004. The correlated inter-annual variations of mesospheric N_2O

and electron fluxes hint at an implication of EEP in the production of N_2O. On the other hand, no temporal correlation of the N_2O evolution with the short-term fluctuations in any of the electron fluxes is visible. This suggests that a dominant local contribution of an EEP-related source at altitudes as low as 58 km is rather unlikely.

5   N_2O enhancements of mesospheric origin seem to occur always in presence of elevated NO_2, although the observed NO_2 vmrs vary drastically from winter to winter (see Figs. 7 and 8, upper panels). This could hint at an implication of NO_2 in the chemical production of N_2O. On the other hand, mesospheric NO_2 enhancements during polar winters are known to be generated by descent of upper atmospheric NO_x produced by
10   energetic particle precipitation (Callis et al., 1998; Siskind, 2000; Funke et al., 2005; Randall et al., 2007). Then, the simultaneous occurrence of both species could simply reflect that their sources are located above the observed altitude (58 km) and their descended contributions are modulated by the meridional circulation in the same manner. A common modulation of N_2O and NO_2 by variable descent velocities and horizontal
15   mixing is further supported by the good temporal correlation of small-scale structures in the evolution of both species which, in turn, is anti-correlated with the evolution of CH_4 vmrs. It is also evident from Figs. 7 and 8 that polar winter enhancements of N_2O are by far not proportional to the available NO_2 amounts. The average N_2O/NO_2 ratios observed during the periods with strongest N_2O enhancements, i.e. in June – August
20   2003 in the SH and January – March 2004 in the NH, were considerably smaller than those observed in periods with weak N_2O enhancements. Further, mesospheric N_2O enhancements tended to start earlier and lasted longer than the NO_2 enhancements.

In order to qualitatively assess the relative magnitudes and peak altitudes of the EEP-related N_2O sources, we have estimated N_2O production rates due to Reactions (R1)
25   and (R2) for different atmospheric conditions.

$N(^4S)$ is generated in presence of EEP by a chain of ionization processes from N_2. It is commonly assumed that each ion pair produced by electron impact leads to the formation of 0.55 $N(^4S)$ atoms (e.g., Jackman et al., 2005). During night, this mechanism represents the only source of $N(^4S)$, while at daytime, NO photolysis leads to

additional N production. The dominating losses of atomic nitrogen are

$$N + NO \rightarrow N_2 + O, \tag{R3}$$

$$N + O_2 \rightarrow NO + O, \tag{R4}$$

and Reaction (R1). Assuming atomic nitrogen to be in steady state and an efficiency of Reaction (R1) to form N_2O of 0.5 (Funke et al., 2008), the N_2O production rate P_1 due to Reaction (R1) is

$$P_1 = \frac{0.5 \times (0.55p + J_{NO}[NO]) \times k_1[NO_2]}{k_3[NO] + k_4[O_2] + k_1[NO_2]}, \tag{2}$$

where p is the ion pair production rate, J_{NO} the photolysis rate of NO, and k_1, k_3, and k_4 are the rate coefficients for the atomic nitrogen loss Reactions (R1), (R3), and (R4), respectively.

$N_2(A^3\Sigma_u^+)$ is also produced by the impact of precipitating electrons. Quenching by atomic oxygen, i.e.

$$N_2(A^3\Sigma_u^+) + O \rightarrow N_2 + O, \tag{R5}$$

and radiative emissions in the Vegard-Kaplan bands with an Einstein coefficient of $0.52\,\mathrm{s}^{-1}$ are the prominent losses in the thermosphere, while at lower altitudes Reaction (R2) becomes dominant. As reported by Zipf and Prasad (1980), we assume that each ion pair produces 0.35 metastable $N_2(A^3\Sigma_u^+)$ molecules. In accordance with the more recent laboratory work of de Sousa et al. (1985), we apply an efficiency of 0.02 to form N_2 in Reaction (R2) as an upper limit. The N_2O production rate P_2 due to Reaction (R2) is then

$$P_2 = \frac{0.02 \times 0.35p \times k_2[O_2]}{k_2[O_2] + k_5[O] + 0.52}, \tag{3}$$

where k_2 and k_5 are the rate coefficients for the Reactions (R2) and (R5), respectively.

As a representative profile of atmospheric ionization due to EEP, we took the average ion pair formation rates calculated by Callis et al. (1998) from MEPED data taken in the period 1979–1987 (see Fig. 2a of their work). These rates might underestimate the EEP-induced ionisation for conditions of elevated geomagnetic activity as encountered during 2003. On the other hand, due to the averaging over nearly an entire solar cycle, they are useful for the estimation of an average N_2O production to be expected during any polar winter. Calculations of the N_2O production rates have been performed for different scenarios of polar winter NO_x descent. In the nominal scenario, NO_x abundances are 20 ppbv at 50 km and increase to 800 ppbv at 75 km (10 ppmv at 100 km). The "high NO_x" scenario reflects the NO_x abundances observed in February 2004 when the unusual descent of upper atmospheric air occurred in the NH polar vortex. In agreement with observations of ACE-FTS (Rinsland et al., 2006) and MIPAS (Funke et al., 2007), we have assumed in this scenario 100 ppbv at 50 km, increasing to 4 ppbv at 75 km (20 ppmv at 100 km). The NO_x partitioning was taken from WACCM model calculations (Garcia et al., 2007) for January, 90° N (polar night) and 60° N at noon (i.e. 80°SZA). In these simulations, the polar night NO_x partitioning in the mesosphere shows only small inter- and intra-annual variations. Nominal temperatures were taken from NRLMSISE-00 (Picone et al., 2002) for January, 90° N. We also included an additional temperature scenario for "strong descent" conditions which reflects the thermal structure over the North pole during end of January 2004, when temperatures 30 K higher (40 K lower) than MSIS were observed at 70 km (50 km) by the SABER instrument (Hauchecorne et al., 2007). Profiles of temperature and vmrs of NO and NO_2 for the different scenarios are shown in Fig. 9. Atomic oxygen densities required for the calculation of P_2 have been taken from WACCM calculations for January, 90°N. Rate constants for Reactions (R1–4) were taken from Sander et al. (2006), while the quenching rate k_5 of Reaction (R5) was taken from Zipf and Prasad (1980).

Figure 10 shows the estimated N_2O production rates P_1 and P_2 due to Reactions (R1) and (R2), respectively, in the presence of EEP. Apart of the nominal scenario, P_1 is also shown for the "high NO_x" scenario combined with the nominal and the "strong descent"

temperature scenarios. Since P_1 depends on illumination, both, polar night and sun overhead conditions have been considered. N_2O production due to Reaction (R2) are independent on temperature and the NO_x abundance. Thus, we have considered the nominal scenario only for the estimation of P_2.

5   The peak nighttime production rate P_1 due to Reaction (R1), located around 73 km, is on the order of $15\,cm^{-3}\,s^{-1}$ (see Fig. 10). The daytime contribution of this reaction has its maximum around 55 km with a N_2O production rate considerably smaller than the corresponding nighttime contribution. This is expected, since daytime NO_2 abundances are very small due to NO_2 photolysis. Daytime N concentrations are driven

10 by NO photolysis rather than by electron impact, which induces a pronounced dependence of P_1 on the NO_x availability during day (compare dashed and solid red line in Fig. 10). This dependence on NO_x is, however, negligible at the P_1 peak height, around 73 km, during night. The reason is that for the atmospheric conditions there, atomic nitrogen losses are dominated by Reactions (R1) and (R3), both involving NO_x. In con-

15 sequence, the N_2O production is mainly driven by the ionization rate and the NO/NO_2 partitioning, there. The latter, however, is expected to introduce only a small variability of P_1. At altitudes below the peak height, the nighttime production rate P_1 depends more strongly on the NO_x vmr, since atomic nitrogen losses due to Reaction (R4) are getting more important towards lower altitudes. An 800% increase of NO_x in the "high

20 NO_x" scenario compared to the nominal scenario results in a 50% increase in the N_2O production at 60 km.

Temperature also affects the N_2O production by Reaction (R1). This is related to the strong temperature dependence of the atomic nitrogen losses by Reaction (R4), leading to a loss at temperatures around 255 K faster by one order of magnitude compared

25 to temperatures around 220 K. When considering the "strong descent" temperature scenario, reflecting the conditions during the Arctic mid-winter 2004, the P_1 profiles are significantly increased below 63 km and slightly decreased above, compared to the nominal temperature scenario (compare dotted and dashed lines in Fig. 10).

For the interpretation of the observed N_2O enhancements in terms of possible pro-

duction by Reaction (R1), it is necessary to assess the dependence of P_1 during night on both temperature and NO_x availability in more detail. Therefore, we have performed calculations of P_1 for various temperatures between 220 and 270 K and NO_x vmrs up to 4 ppmv (not shown). It turned out that for typical polar winter temperatures of 220 K

5 at 70 km, P_1 is rather proportional to NO_x up to approximately 20 ppbv, while for NO_x abundances larger than 100 ppbv the impact of the NO_x abundance on P_1 is weak. NO_x abundances of more than 100 ppbv are generally found above 70 km during typical polar winters. For perturbed temperatures of 255 K, the linear dependence on NO_x is extended up to 150 ppbv. The region of weak NO_x dependence starts at NO_x

10 vmrs around 500 ppbv. Since such high temperatures are generally found in winters with strong subsidence and hence high NO_x availability, P_1 is expected to be rather independent on NO_x at its peak height also in presence of high temperatures.

The maximum of the production rate P_2 is located at 95–100 km with a magnitude of 25 $cm^{-3} s^{-1}$ and decreasing to values smaller than 1 $cm^{-3} s^{-1}$ below 75 km. P_2 is

15 mainly driven by the EEP ionization rate, though above 90 km, increasing atomic oxygen densities make P_2 dependent on the O/O_2 partitioning. At the P_2 peak height, around half of the EEP-generated $N_2(A^3\Sigma_u^+)$ molecules are quenched by atomic oxygen before they can react with O_2 to form N_2O.
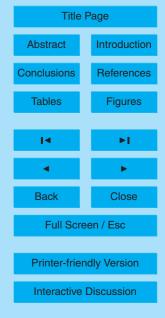
Despite this dependence on the O/O_2 partitioning, N_2O production by Reaction (R2)

20 shows similarities with the EEP-induced NO production in terms of both source region and variability. The magnitude of the NO production, however, is higher than our estimates of the N_2O production by Reaction (R2) by approximately a factor of 200, assuming that 0.7 NO molecules are produced by each ion pair (Jackman et al., 2005). In consequence, we would expect that during polar winter, when photochemical losses

25 are small, the N_2O produced by Reaction (R2) is about 0.5% of the NO_x abundance in air masses descended from the upper atmosphere.

During mid winter, the average polar NO_2 abundances at 58 km, as shown in Figs. 7 and 8, represent a good proxy of total NO_x. During the 2002 Antarctic and 2002/2003 Arctic winters, observed NO_2 abundances at 58 km were generally lower than 15 ppbv.

Hence, a negligible contribution by Reaction (R2) to the observed N_2O enhancements of less than 0.07 ppbv would be expected at this altitude. However, during the Antarctic winter 2003, when NO_2 abundances of more than 100 ppbv were measured, this contribution could have made up to 0.5 ppbv, which is about 40% of the N_2O enhancements observed in this period. During January–March 2004 in the Arctic, the contribution due to Reaction (R2) could have even been as high as 1.5 ppbv which makes up 25% of the observed N_2O enhancements. We recall, however, that these estimates represent an upper limit for a possible contribution of Reaction (R2).

In the lower thermosphere, N_2O abundances on the order of several 100 ppbv would then be expected due to Reaction (R2). Unfortunately, there are no thermospheric N_2O measurements available which would support such high N_2O amounts. We thus have looked at MIPAS spectra taken in the upper atmospheric observation mode on 11 June 2003, which includes tangent heights up to 100 km. No evidence for N_2O emissions at tangent heights around 90–100 km was found in any of the N_2O bands included in the MIPAS spectra. However, due to the low signal-to-noise ratio at these altitudes, only N_2O abundances higher than approximately 200 ppbv could have been detected by MIPAS at these tangent heights.

In this sense, a possible contribution of Reaction (R2) can neither be proven nor excluded. In any case, even when assuming a maximum efficiency of this reaction to form N_2O, its contribution could only explain a small fraction of the observed N_2O enhancements.

Assuming a continuous EEP-induced N_2O production with typical rates as provided by our estimates of P_1 and a transport-limited N_2O lifetime of a few weeks, Reaction (R1) would lead to N_2O abundances on the order of several ppbv at its source region around 70 km. Since our estimations reflect conditions of average geomagnetic activity, even higher mesospheric N_2O abundances would be found in periods of elevated geomagnetic activity, e.g. during the Antarctic winter 2003 and Arctic winter 2004. Although N_2O abundances are expected to decrease towards lower altitudes due to dilution during the descent, it seems plausible that N_2O abundances such as observed at

58 km during the 2002–2004 polar winters could have been caused by Reaction (R1). It has already been demonstrated by CMAM model calculations (Semeniuk et al., 2007)[1], that a dominant contribution to the mesospheric N_2O enhancements during the Arctic winter 2004 was generated by this reaction during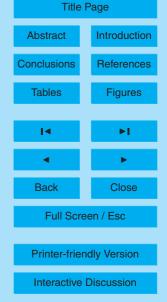 night. It is thus very likely, that its nighttime contribution was also responsible for the major part of the N_2O enhancements observed in the other polar winters. Its daytime contribution, which does not require the presence of EEP, is expected to be considerably smaller. Nevertheless, minor N_2O amounts could have been produced in illuminated regions at altitudes below 60 km, in particular during winters with high NO_x availability (i.e., February 2004). A dominant nighttime contribution originated from a source region around 70–75 km is also supported by the finding that the observed N_2O enhancements at 58 km are more efficiently modulated by dynamical factors than by the electron flux variability.

As demonstrated above, nighttime N_2O production by Reaction (R1) is mainly driven by the EEP-induced ionisation rate around 73 km. Hence, except for dynamical modulations, the inter-annual variations of the observed polar winter N_2O enhancements should be correlated to the flux variations of precipitating electrons with energies greater than 100 keV. Indeed, we found the highest N_2O amounts in the 2003 SH and 2004 NH winters with most elevated fluxes of $a>100$ keV electrons. However, it is striking that the N_2O enhancements observed during the 2003 SH winter at 58 km were about 5 times smaller than those of the 2004 NH winter, although the observed >100 keV electron fluxes were comparable. This apparent asymmetry could be explained by the unusually strong polar vortex during the 2004 NH winter leading to a more efficient descent of N_2O produced around 73 km than in the 2003 SH winter. Further, favored by the low temperatures and high NO_x availability, significant N_2O production could have occurred at altitudes below 65 km during the 2004 NH winter.

We have further observed that the N_2O/NO_2 ratio tended to be considerably higher at the beginning and the end of the polar winters. As discussed above, the non-linear dependence of the nighttime fraction of P_1 on the NO_x availability could be responsible for variations of the N_2O/NO_2 ratio: At the beginning and the end of the winter, when
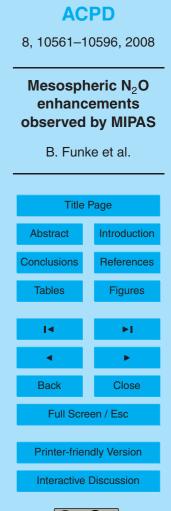
only small amounts of NO_x are available, N_2O increases linearly with NO_2, while during mid winter, sufficient NO_x is available to make the N_2O production dependent on the EEP-induced ionization and the NO_x partitioning, only.

In summary, we have shown that the magnitude and temporal evolution of the observed N_2O enhancements during the 2002–2004 polar winters are in concordance with a dominant nighttime N_2O source around 73 km due to Reaction (R1) which is driven by energetic electron precipitation. The variability of N_2O at 58 km over various winters seems to be driven by both dynamical conditions and variations of the source strength. Further, we cannot exclude that Reaction (R2) contributed additionally by up to 25–40% to the observed enhancements.

5 Conclusions

We have presented observations of enhanced N_2O abundances, ranging from 0.5 to 6 ppbv in the polar upper stratosphere/lower mesosphere, which have been taken by the MIPAS instrument on the Envisat satellite during the Arctic and Antarctic winters in the period July 2002–March 2004. These N_2O enhancements have been found in two data sets resulting from independent processing, the first, generated at IMK/IAA, and the second, generated by the operational data processing performed by ESA. The good agreement of both data sets makes is unlikely that the observed N_2O enhancements are related to retrieval artifacts.

Simultaneous N_2O and CH_4 observations show a pronounced anti-correlation during polar winters at CH_4 levels lower than 0.1 ppmv. This behavior gives clear evidence that the N_2O enhancements are of chemical rather than dynamical origin. As a consequence, polar winter N_2O-CH_4 correlations should be used with caution in tracer-tracer studies due to the perturbations by this mesospheric N_2O source.

The finding that chemical production of N_2O occurred in the mesosphere during all polar winters in the period 2002–2004, though with variable magnitude, makes it rather unlikely that mesospheric N_2O enhancements are infrequent isolated phenomena.

Full Screen / Esc

Printer-friendly Version

Interactive Discussion

The polar winter N_2O enhancements observed at 58 km occurred in the presence of NO_x intrusions from the upper atmosphere which were related to energetic particle precipitation. Further, the inter-annual variability of mesospheric N_2O correlates well with precipitating electron fluxes as measured by the MEPED instrument. On the other hand, we found a pronounced anti-correlation of the temporal evolutions of N_2O and CH_4 at 58 km, which hints at a dynamical modulation of descending N_2O from a source region at higher altitudes.

The analysis of possible chemical production mechanisms shows that the major part of the observed N_2O enhancements is most likely generated under dark conditions by the reaction of NO_2 with atomic nitrogen in the presence of energetic particle precipitation. N_2O production due to this mechanism has its maximum around 73 km. The polar winter N_2O abundances observed at 58 km seem to be modulated by both variations of the source strength and dynamical factors driving the efficiency of the descent from the source region. An additional source of N_2O in the middle and upper polar atmosphere could represent the reaction of $N_2(A^3\Sigma_u^+)$, generated by precipitating electrons, with O_2, which would lead to N_2O production peaking at altitudes around 90–100 km. N_2O produced by the latter mechanism could have then descended to the upper stratosphere and mesosphere during the 2002–2004 polar winters, where it could have contributed to the observed N_2O enhancements by up to 25–40%.

EEP-generated mesospheric N_2O represents a continuous, though variable, source of stratospheric odd nitrogen during polar winters. This source, however, is of minor importance when comparing to EEP-induced NO production.

Mesospheric N_2O enhancements observed by MIPAS

B. Funke et al.

Title Page

Abstract | Introduction

Conclusions | References

Tables | Figures

◄ | ►

◄ | ►

Back | Close

Full Screen / Esc

Printer-friendly Version

Interactive Discussion

References

Callis, L. B., Natarajan, M., Lambeth, J. D., and Baker, D. N.: Solar atmospheric coupling by electron (SOLACE 2. Calculated stratospheric effects of precipitationg electron, 1979–1988, J. Geophys. Res., 103, 28 421–28 438, 1998. 10573, 10574, 10576

de Sousa, A. R., Touzeau, M., and Petitdidier, M.: Quenching reactions of metastable $N_2(A^3\Sigma, v = 0, 1, 2)$ molecule with O_2, Chem. Phys. Lett., 121, 1985. 10563, 10575

Echle, G., von Clarmann, T., Dudhia, A., Flaud, J.-M., Funke, B., Glatthor, N., Kerridge, B., López-Puertas, M., Martín-Torres, F. J., and Stiller, G. P.: Optimized spectral microwindows for data analysis of the Michelson Interferometer for Passive Atmospheric Sounding on the Environmental Satellite, Appl. Opt., 39, 5531–5540, 2000. 10565

European Space Agency: Envisat, MIPAS An instrument for atmospheric chemistry and climate research, ESA Publications Division, ESTEC, P. O. Box 299, 2200 AG Noordwijk, The Netherlands, SP-1229, 2000. 10564

Fischer, H. and Oelhaf, H.: Remote sensing of vertical profiles of atmospheric trace constituents with MIPAS limb-emission spectrometers, Appl. Opt., 35, 2787–2796, 1996. 10564

Fischer, H., Birk, M., Blom, C., Carli, B., Carlotti, M., von Clarmann, T., Delbouille, L., Dudhia, A., Ehhalt, D., Endemann, M., Flaud, J. M., Gessner, R., Kleinert, A., Koopmann, R., Langen, J., López-Puertas, M., Mosner, P., Nett, H., Oelhaf, H., Perron, G., Remedios, J., Ridolfi, M., Stiller, G., and Zander, R.: MIPAS: an instrument for atmospheric and climate research, Atmos. Chem. Phys. Discuss., 7, 8795–8893, 2007, http://www.atmos-chem-phys-discuss.net/7/8795/2007/. 10564

Funke, B., López-Puertas, M., Gil-López, S., von Clarmann, T., Stiller, G. P., Fischer, H., and Kellmann, S.: Downward transport of upper atmospheric NO_x into the polar stratosphere and lower mesosphere during the Antarctic 2003 and Arctic 2002/2003 winters, J. Geophys. Res., 110, D24308, doi:10.1029/2005JD006463, 2005. 10567, 10574

Funke, B., López-Puertas, M., Fischer, H., Stiller, G. P., von Clarmann, T., Wetzel, G., Carli, B., and Belotti, C.: Comment on 'Origin of the January–April 2004 increase in stratospheric NO_2 observed in northern polar latitudes' by J.-B. Renard et al., Geophys. Res. Lett., 34, L07813, doi:10.1029/2006GL027518, 2007. 10576

Funke, B., García-Comas, M., López-Puertas, M., Glatthor, N., Stiller, G. P., von Clarmann, T., Semeniuk, K., and McConnell, J. C.: Enhancement of N_2O during the October-November 2003 solar proton events, Atmos. Chem. Phys. Discuss., 8, 4669–4691, 2008,

Mesospheric N_2O enhancements observed by MIPAS

B. Funke et al.

Title Page

Abstract	Introduction
Conclusions	References
Tables	Figures

◄◄	►►
◄	►
Back	Close

Full Screen / Esc

Printer-friendly Version

Interactive Discussion

http://www.atmos-chem-phys-discuss.net/8/4669/2008/. 10563, 10568, 10573, 10575

Garcia, R. R., Marsh, D. R., Kinnison, D. E., Boville, B. A., and Sassi, F.: Simulation of secular trends in the middle atmosphere, J. Geophys. Res., 112, D09301, doi:10.1029/2006JD007485, 2007. 10576

5 Glatthor, N., von Clarmann, T., Fischer, H., Funke, B., Grabowski, U., Höpfner, M., Kellmann, S., Kiefer, M., Linden, A., Milz, M., Steck, T., Stiller, G. P., Mengistu Tsidu, G., and Wang, D. Y.: Mixing processes during the Antarctic vortex split in September/October 2002 as inferred from source gas and ozone distributions from ENVISAT-MIPAS, J. Atmos. Sci., 62, 787–800, 2005. 10565

10 Hauchecorne, A., Bertaux, J.-L., Dalaudier, F., Russell III, J. M., Mlynczak, M. G., Kyrölä, E., and Fussen, D.: Large increase of NO_2 in the north polar mesosphere in January–February 2004: Evidence of a dynamical origin from GOMOS/ENVISAT and SABER/TIMED data, Geophys. Res. Lett., 34, L03810, doi:10.1029/2006GL027628, 2007. 10576

Iannuzzi, M. P., Jeffries, J. B., and Kaufman, F.: Product channels of the $N_2(A^3\Sigma_u^+)+O_2$ interac-
15 tion, Chem. Phys. Lett., 87, 570–574, 1982. 10563

Jackman, C. H., DeLand, M. T., Labow, G. J., Fleming, E. L., Weisenstein, D. K., Ko, M. K. W., Sinnhuber, M., and Russell, J. M.: Neutral atmospheric influences of the solar proton events in October–November 2003, J. Geophys. Res., 110, A09S27, doi:10.1029/2004JA01088, 2005. 10574, 10578

20 Jackman, C. H., Marsh, D. R., Vitt, F. M., Garcia, R. R., Fleming, E. L., Labow, G. J., Randall, C. E., López-Puertas, M., Funke, B., von Clarmann, T., and Stiller, G. P.: Short- and medium-term atmospheric effects of very large solar proton events, Atmos. Chem. Phys., 8, 765–785, 2008, http://www.atmos-chem-phys.net/8/765/2008/. 10572, 10593

Manney, G. L., Krüger, K., Sabutis, J. L., Sena, S. A., and Pawson, S.: The remarkable 2003–
25 2004 winter and other recent warm winters in the Arctic stratosphere since the late 1990s, J. Geophys. Res., 110, D04107, doi:10.1029/2004JD005367, 2005. 10567

Michelsen, H. A., Manney, G. L., Gunson, M. R., Rinsland, C. P., and Zander, R.: Correlations of stratospheric abundances of CH_4 and N_2O derived from ATMOS measuremets, Geophys. Res. Lett., 25, 2777–2780, 1998a. 10562, 10570

30 Michelsen, H. A., Manney, G. L., Gunson, M. R., and Zander, R.: Correlations of stratospheric abundances of NO_y, O_3, N_2O, and CH_4 derived from ATMOS measurements, J. Geophys. Res., 103, 28 347–28 359, 1998b. 10570

Nett, H., Carli, B., Carlotti, M., Dudhia, A., Fischer, H., Flaud, J.-M., Perron, G., Raspollini,

P., and Ridolfi, M.: MIPAS Ground Processor and Data Products, in: Proc. IEEE 1999 International Geoscience and Remote Sensing Symposium, 28 June–2 July 1999, Hamburg, Germany, 1692–1696, 1999. 10564

Nett, H., Perron, G., Sanchez, M., Burgess, A., and Mosner, P.: MIPAS in-flight calibration and processor verification, in: ENVISAT Calibration Review – Proc. of the European Workshop, 9–13 September 2002, ESTEC, Noordwijk, The Netherlands, CD-ROM, edited by: Sawaya-Lacoste, H., vol. SP-520, ESA Publications Division, ESTEC, Postbus 299, 2200 AG Noordwijk, The Netherlands, 2002. 10564

Newman, P. A. and Nash, E. R.: The Unusual Southern Hemisphere Stratosphere Winter of 2002, J. Atmos. Sci., 62, 614–628, 2005. 10567

Picone, J., Hedin, A., Drob, D., and Aikin, A.: NRLMSISE-00 empirical model of the atmosphere: Statistical comparisons and scientific issues, J. Geophys. Res., 107, 1468, doi:10.1029/2002JA009430, 2002. 10576

Plumb, R. A., Waugh, D. W., and Chipperfield, M. P.: The effects of mixing on tracer relationships in the polar vortices, J. Geophys. Res., 105, 10 047–10 062, 2000. 10562

Randall, C. E., Harvey, V. L., Singleton, C. S., Bailey, S. M., Bernath, P. F., Codrescu, M., Nakajima, H., and Russell III, J. M.: Energetic particle precipitation effects on the Southern Hemisphere stratosphere in 1992–2005, J. Geophys. Res., 112, D08308, doi: 10.1029/2006JD007696, 2007. 10574

Raspollini, P., Belotti, C., Burgess, A., Carli, B., Carlotti, M., Ceccherini, S., Dinelli, B. M., Dudhia, A., Flaud, J.-M., Funke, B., Höpfner, M., López-Puertas, M., Payne, V., Piccolo, C., Remedios, J. J., Ridolfi, M., and Spang, R.: MIPAS level 2 operational analysis, Atmos. Chem. Phys., 6, 5605–5630, 2006, http://www.atmos-chem-phys.net/6/5605/2006/. 10569

Ray, E. A., Moore, F. L., Elkins, J. W., Hurst, D. F., Romashkin, P. A., S.Dutton, G., and Fahey, D. W.: Descent and mixing in the 1999–2000 northern polar vortex inferred from in situ tracer measurements, J. Geophys. Res., 107, 8285, doi:10.1029/2001JD000961, 2002. 10563

Rinsland, C. P., Goldman, A., Elkins, J. W., Chiou, L. S., Hannigan, J. W., Wood, S. W., Mahieu, E., and Zander, R.: Long–term trend of CH_4 at northern mid–latitudes: Comparison between ground–based infrared solar and surface sampling measurements, J. Quant. Spectrosc. Ra., 97, 457–466, doi:10.1016/j.jqsrt.2005.07.002, 2006. 10576

Sander, S. P., Friedl, R. R., Ravishankara, A. R., Golden, D. M., Kolb, C. E., Kurylo, M. J., Molina, M. J., Moortgat, G. K., Keller-Rudek, H., Finlayson-Pitts, B. J., Wine, P., Huie, R. E., and Orkin, V. L.: Chemical kinetics and Photochemical Data for the Use in Atmospheric Stud-

Mesospheric N_2O enhancements observed by MIPAS

B. Funke et al.

ies. Evaluation Number 15, JPL publication 06-2, Jet Propulsion Laboratory, 2006. 10576

Siskind, D. E.: Atmospheric science across the Stratopause, 123 of Geophysical Monograph, chap. On the coupling between middle and upper atmospheric odd nitrogen, 101–116, American Geophysical Union, 2000. 10574
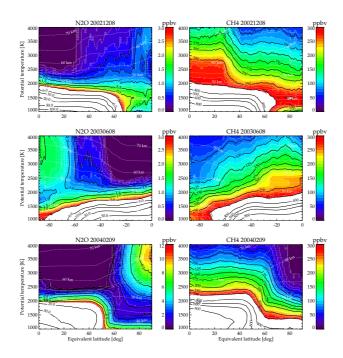
5 Stiller, G. P., von Clarmann, T., Funke, B., Glatthor, N., Hase, F., Höpfner, M., and Linden, A.: Sensitivity of trace gas abundances retrievals from infrared limb emission spectra to simplifying approximations in radiative transfer modelling, J. Quant. Spectrosc. Ra., 72, 249–280, 2002. 10565

von Clarmann, T., Chidiezie Chineke, T., Fischer, H., Funke, B., García-Comas, M., Gil-López,
10 S., Glatthor, N., Grabowski, U., Höpfner, M., Kellmann, S., Kiefer, M., Linden, A., López-Puertas, M., López-Valverde, M. Á., Mengistu Tsidu, G., Milz, M., Steck, T., and Stiller, G. P.: Remote Sensing of the Middle Atmosphere with MIPAS, in: Remote Sensing of Clouds and the Atmosphere VII, edited by: Schäfer, K., Lado-Bordowsky, O., Comerón, A., and Picard, R. H., 4882, 172–183, SPIE, Bellingham, WA, USA, 2003a. 10565

15 von Clarmann, T., Glatthor, N., Grabowski, U., Höpfner, M., Kellmann, S., Kiefer, M., Linden, A., Mengistu Tsidu, G., Milz, M., Steck, T., Stiller, G. P., Wang, D. Y., Fischer, H., Funke, B., Gil-López, S., and López-Puertas, M.: Retrieval of temperature and tangent altitude pointing from limb emission spectra recorded from space by the Michelson Interferometer for Passive Atmospheric Sounding (MIPAS), J. Geophys. Res., 108, 4736, doi:10.1029/2003JD003602,
20 2003b. 10565

Zipf, E. C.: A laboratory study on the form of nitrous oxide by the reaction $N_2(A^3\Sigma_u^+)+O_2 \rightarrow N_2O+O$, Nature, 287, 523–524, 1980. 10563

Zipf, E. C. and Prasad, S.: Production of nitrous oxide in the auroral D and E regions, Nature, 287, 525–526, 1980. 10563, 10575, 10576

Mesospheric N$_2$O enhancements observed by MIPAS

B. Funke et al.

Title Page

Abstract	Introduction
Conclusions	References
Tables	Figures

|◄ | ►|

◄ | ►

Back | Close

Full Screen / Esc

Printer-friendly Version

Interactive Discussion

Fig. 1. Potential temperature-equivalent latitude daily mean cross sections of N$_2$O (left) and CH$_4$ (right) vmr retrieved by IMK/IAA for the NH for 8 December 2002 (top), SH for 8 June 2003 (middle), and NH for 9 February 2004 (bottom). Data versions used are V3O_8.0 (top and middle) and V3O_12.0 (bottom). Mean geometric heights are indicated by dotted white lines. Note the different scale in the bottom left panel.
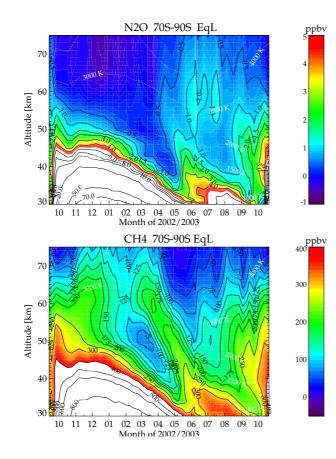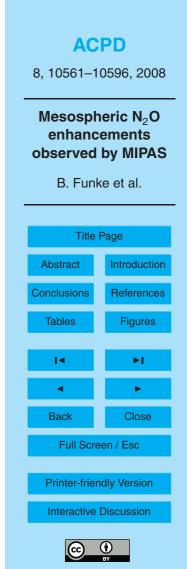
Fig. 2. Temporal evolution of N$_2$O (top) and CH$_4$ (bottom) VMR retrieved by IMK/IAA (Version V3O_8.0) averaged over equivalent latitudes 70–90° S from September 2002 until October 2003. An area-weighting factor (cosine of equivalent latitude) has been applied. Mean potential temperatures are indicated by dotted white lines.

Fig. 3. As Fig. 2, but for equivalent latitudes 70–90° N.

Fig. 4. Temporal evolution of N$_2$O (top) and CH$_4$ (bottom) VMR retrieved by IMK/IAA (Version V3O_12.0) averaged over equivalent latitudes 70–90° N from September 2003 until March 2004. An area-weighting factor (cosine of equivalent latitude) has been applied. Mean potential temperatures are indicated by dotted white lines.

Fig. 5. 70–90° S (top) and 70–90° N (bottom) averages of ESA N$_2$O vmr (reprocessed data version 4.61/4.62) with and without statistical correction (black and red solid lines, respectively), single measurement noise errors (green solid line), and N$_2$O vmr retrieved at IMK/IAA (Versions V3O_8.0 and V3O_12.0 shown by red and blue diamonds, respectively) at 58 km. Spikes in the N$_2$O averages on 26 September 2002 (SH), 29 April 2003 (NH), and 29 July 2003 (NH) are generated by spurious data.

Fig. 6. Monthly mean median values of N$_2$O PDFs at given CH$_4$ levels calculated from ESA 4.61/4.62 data products for 60–90° S (top) and 60–90° N (bottom). White regions reflect an availability of less then 30 observations at the corresponding CH$_4$ level. Note the different color scales for SH and NH!
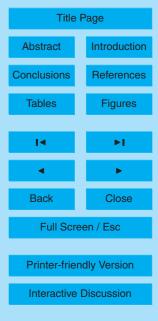
Fig. 7. Upper panel: Smoothed temporal evolution of the estimated mesospheric (solid red) and tropospheric (dotted blue) contributions to the observed N$_2$O vmr, as well as NO$_2$ (solid green) and CH$_4$ (dotted black) vmrs (corrected ESA data) at 58 km averaged over 70–90° S. Note that NO$_2$ and CH$_4$ vmrs are scaled by a factor of 0.02. Lower panels: 30-day averages of integral precipitating electron fluxes within L>2.5 and 60–90° S with energies >30 keV (red), >100 keV (green), and >300 keV (blue) as measured by the MEPED instrument on NOAA. Atmospheric ionization rates at 0.3 hPa due to solar protons from Jackman et al. (2008) are also shown (black). Units are arbitrary.
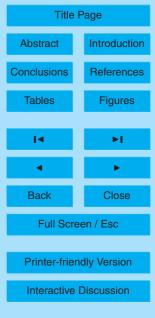
Fig. 8. As Fig. 7, but for 70–90° N.

Fig. 9. Left: Kinetic temperatures used in the nominal (solid line) and "strong descent" (dotted line) scenario. Right: Volume mixing ratios of NO$_2$ and NO during polar night (solid and dotted lines, respectively) and NO$_2$ during day (dashed line) used in the nominal (black) and in the "high NO$_x$" scenario (red).
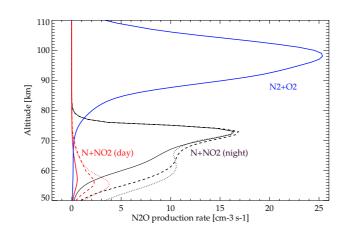
Fig. 10. Estimated EEP-related N$_2$O productions by Reaction (R1) at polar night (solid black line) and day (SZA=80°) conditions (solid red line), as well as by Reaction (R2) (solid blue line) for the nominal scenario. Dashed and dotted lines represent N$_2$O productions for the "high NO$_x$" scenario combined with the nominal and the "strong descent" temperature scenarios, respectively (only Reaction R1). See text for further details.